POLSKA AKADEMIA NAUK
INSTYTUT MASZYN PRZEPŁYWOWYCH

TRANSACTIONS OF THE INSTITUTE OF FLUID-FLOW MACHINERY

PRACE INSTYTUTU MASZYN PRZEPŁYWOWYCH

101

WYDAWNICTWO IMP PAN

GDAŃSK 1996

THE TRANSACTIONS OF THE INSTITUTE OF FLUID-FLOW MACHINERY

exist for the publication of theoretical and experimental investigations of all aspects of the mechanics and thermodynamics of fluid-flow with special reference to fluid-flow machines

*

PRACE INSTYTUTU MASZYN PRZEPŁYWOWYCH

poświęcone są publikacjom naukowym z zakresu teorii i badań doświadczalnych w dziedzinie mechaniki i termodynamiki przepływów, ze szczególnym uwzględnieniem problematyki maszyn przepływowych

Wydanie publikacji dofinansowane zostało przez PAN ze środków DOT uzyskanych z Komitetu Badań Naukowych

EDITORIAL OFFICE – REDAKCJA

Wydawnictwo Instytutu Maszyn Przepływowych
Polskiej Akademii Nauk
ul. Gen. Józefa Fiszera 14, 80-952 Gdańsk, skr. poczt. 621,
☎ (0-58) 46-08-81 wew. 141, fax: (0-58) 41-61-44,
e-mail: esli@imppan.imp.pg.gda.pl

ISSN 0079-3205

TRANSACTIONS OF THE INSTITUTE OF FLUID-FLOW MACHINERY
1996 No. 101

JAN KICIŃSKI[1]

Nonlinear model of vibration in rotor-bearings system. Part II. Calculation results

The results of simulation research related to the description of the most striking and not yet fully explained phenomena occurring in the oil film of slide bearings, namely, the oil whirls and whips have been presented. The calculations were made on the example of a laboratory rotor, based upon two supports with flexible external fixing of the bearing shells, and a 200 MW steam turbine rotor as well. The respective initial phases of the oil vibrations development have been determined in details and an attempt has been made to classify the orbits and to find out a practical diagnostic discriminant.

Nomenclature

A_w – vibration amplitude of the disk centre (half of the longest distance of two points of the trajectory) [m],

$c_{i,k}$ – stiffness coefficients of the oil film [N·m^{-1}]

$d_{i,k}$ – damping coefficients of the oil film [N·s·m^{-1}],

f – frequency [Hz],

f_n – synchronous frequency corresponding to the rotational speed of the rotor n [Hz]; $f_n = n/60$,

$f_w^*, f_{s1}^*, f_{s2}^*$ – oil vibration frequencies of the system corresponding to critical velocities n_{k1}^* and n_{k2}^* [Hz],

i^* – number of rotation markers (number of points along the trajectory corresponding to the position of the unbalance vector for $\tau = 0^o, 360^o, 720^o$),

m_c – disk mass of the two-support rotor [kg],

n – rotational speed of the rotor [rpm],

n_{wp} – speed of the oil "whip" [rpm],

n_{gr} – formal stability threshold of the

q_n – force due to unbalance of the rotating disk [N],

$\hat{r}$ – unbalance radius [m],

ΔR – absolute radial clearance of the bearing [m],

x, y, X, Y – dimensional [m] and non-dimensional system of coordinates $x = x/\Delta R$, $Y = y/\Delta R$,

$\lambda_{i,k}, \lambda_{11}, \lambda_{22}$ – stiffnesses of the external fixing of bearing shells in general; stiffnesses: horizontal and vertically, respectively [Nm^{-1}],

Φ_w, Φ_w^0 – phase angles of the disk centres in general; phase angles for the position of the unbalance vector,

$\Phi_w^{360}, \Phi_w^{720}$ – for $\tau = 0^o, 360^o, 720^o$, respectively [in degrees] (definition of angles is given in Fig. 1c),

τ – angle determining the position of the unbalance vector [in degrees]; $\tau = \omega t$,

θ^* – trajectory period [in degrees],

θ_{pr} – period of registering the results ("sampling" period) [in degrees],

[1]Institute of Fluid-Flow Machinery, Department of Tribology, ul. Fiszera 14, 80-952 Gdańsk

system [rpm],
n^*_{k1}, n^*_{k2} – critical velocities of the system [rpm],
θ_w – period of the force exciting vibration of the system [in degrees],
ω – angular velocity of the rotor [rad s^{-1}].

1. Preliminary remarks

In part I there has been presented a complex nonlinear theoretical model of rotor-bearing-supports system with the applied computer program NLDW-01. There have also been given some examples of experimental verification of the model in the area of the hydrodynamic instability occurrence (small oil vibrations). The experimental tests were performed at a special large-sized test rig. There has been obtained a qualitatively complete set of the theoretical and experimental results, and taking also into consideration the unavoidable technological errors, in particular, regarding to the shape of the bearing lubrication gap, a satisfactory quantitative consistence as well.

On account of operational safety of the test rig and its technical capabilities the verification of the model was impossible within the area of the acquiring large oil vibrations, that is, in the range of the so-called oil "whip". However, it can be assumed that a model providing verified data relevant to stable operation of the system and small oil vibrations will also be a reliable instrument for the analysis of other factors.

Let us follow the way of systematic simulation investigation of the development stages of the specific oil vibrations generated entirely by the hydrodynamic slide bearings. Thereby it will be possible to explain the hydrodynamic instability mechanism being originated in the rotor-bearing-supports system. The simulation investigation will be carried out both on the example of a simple, two-support rotor being the model of rotor used for experimental investigation, and on the example of a large fluid-flow machine (200 MW turbine).

2. Simulation investigation on the example of two-support rotor

Let us concentrate our attention on the development of oil whirls and whip on the example of a two-support rotor shown in Fig. 1a. Let its theoretical projection be the thirteen-mass system given in Fig. 1b (10 finite beam elements, 2 point elements modelling the lubrication film, and 2 point elements modelling the effect of the external fixing of the bearing shells).

Let the shells of the slide bearings of mass 15 kg each be fixed within flexible elements of horizontal stiffness $\lambda_{11} = 0.2 \times 10^8$ N/m and vertical stiffness $\lambda_{22} = 1.2 \times 10^8$ N/m (the cross-coupled stiffness λ_{12} and λ_{21} of fixing, as well as its damping $\Lambda_{i,k}$ will be neglected).

Let us use for the investigation a slide bearing with two lubrication grooves of angular span 20^o each on the bearing shell parting plane, with cylindrical

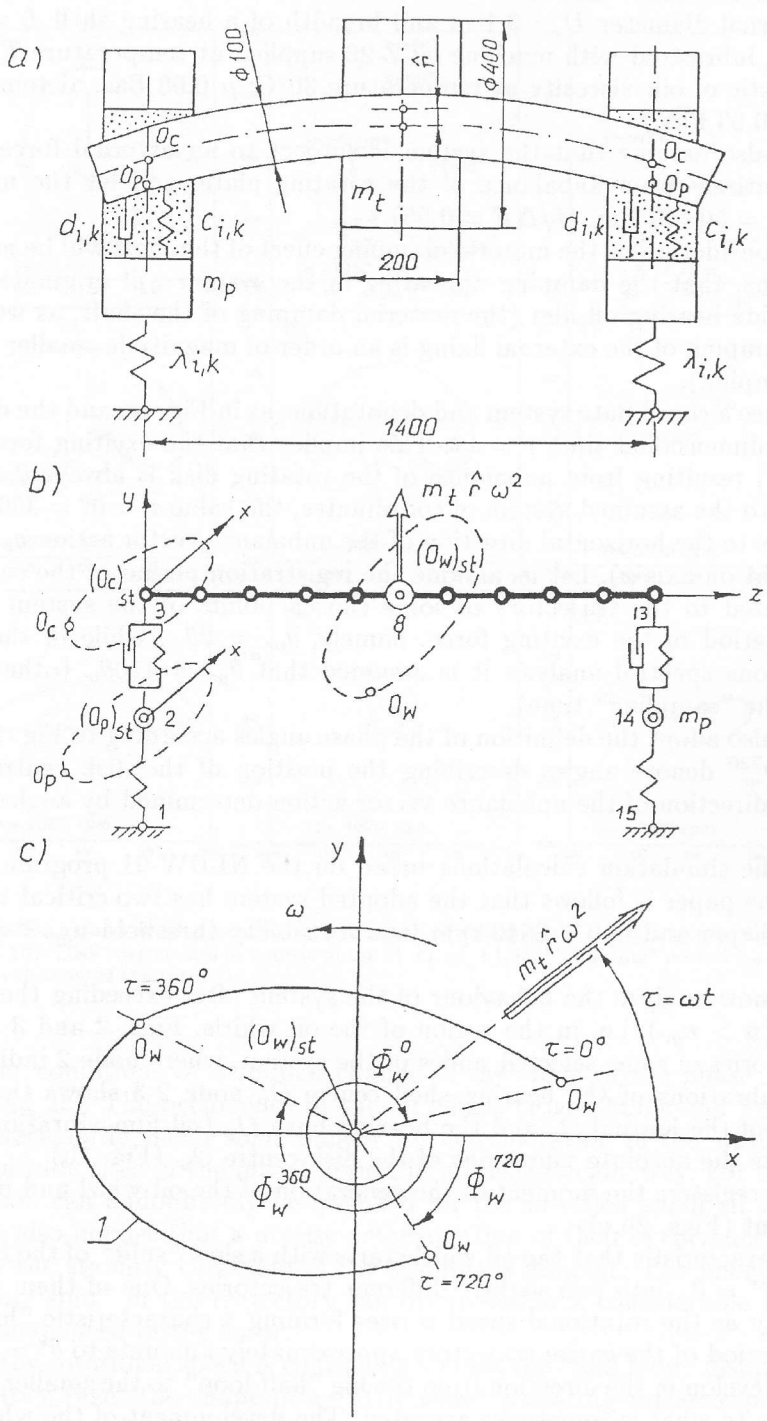

Fig. 1. Model of the rotor-bearing-supports system a) adopted for the simulation investigation and the scheme of its discretization, b) definition of phase angles with reference to the disk centre, c) 1 – trajectory of the disk centre.

clearance of absolute value $\Delta R = 90 \times 10^{-6}$ m (relative clearance $\Delta R/R =$ 1.8‰), journal diameter $D = 0.1$ m and breadth of a bearing shell $L = 0.05$ m $L/D = 0.5$, lubricated with machine oil Z-26 supplied at temperature $T_o = 30^oC$ (characteristic of oil: viscosity at temperature 30^oC: μ 0.08 Pas, at temperature 50^oC: $\mu = 0.03$ Pas.)

Let us also assume that the system is subject to an external force, a force resulting entirely from unbalance of the rotating plate, and let the unbalance radius be $\hat{r} = 50 \cdot 10^{-6}$m, $(\hat{r}/\Delta R = 0.55)$.

In the considerations the material damping effect of the shaft will be neglected, which means, that the damping appearing in the system will originate entirely from the slide bearing oil film (the material damping of the shaft, as well as the material damping of the external fixing is an order of magnitude smaller than the oil film damping).

Let us use a coordinate system and denotations as in Fig. 1c, and the definition of the non-dimensional time $\tau = \omega t$. This implies that the exciting force period (in degrees) resulting from unbalance of the rotating disk is always $\theta_w = 360^o$. According to the assumed system of coordinates, the value $\tau = 0^o = 360^o = 720^o$ corresponds to the horizontal direction of the unbalance vector action $q_n = m\hat{r}\omega^2$ (on the right on axis x). Let us assume the registration period of the calculation results related to the trajectory of some chosen points of the system equal to a double period of the exciting force, namely, $\theta_{pr} = 2\theta_w$, while in the case of the vibrations spectral analysis it is assumed that $\theta_{pr} = 110\theta_w$ (otherwise θ_{pr} indicates the "sampling" time).

Let us also adopt the definition of the phase angles according to Fig. 1c, where $\Phi_w^o, \Phi_w^{360}, \Phi_w^{720}$ denote angles describing the position of the disk centre O_w for horizontal direction of the unbalance vector action determined by angles $\tau_0^o, 360^o$ and 720^o.

From the simulation calculations based on the NLDW-01 program given in Part I of the paper it follows that the adopted system has two critical velocities $n_{k1}^* \cong 2120$ rpm and $n_{k2}^* \cong 2540$ rpm, and a stability threshold $n_{gr} \cong 3650$ rpm (Fig. 5).

Let us now analyze the behaviour of the system after exceeding the stability threshold $(n > n_{gr})$, i.e. in the region of the oil whirls. Figs. 2 and 3 illustrate the trajectories of some selected nodes of the system, where node 2 indicates the absolute vibrations of the bearing shell centre O_p node 2-3 shows the relative vibrations of the journal O_c and the bearing bush O_p (oil film vibrations), node 8 represents the absolute vibrations of the disk centre O_w (Fig. 1b).

Fig. 2a registers the moment of the generation of the oil whirl and its further development (Figs. 2b,c).

It is characteristic that the oil whirl starts with a slow "split" of the trajectory of period $\theta^* = \theta_w$ into two slightly different trajectories. One of them decreases significantly as the rotational speed n rises forming a characteristic "half-loop". Now the period of the entire trajectory approximately amounts to $\theta^* = 2\theta_w$. The oil whirls develop in the direction from the big "half-loop" to the smaller one, that is, contrary to what is sometimes accepted. The development of the whirls takes

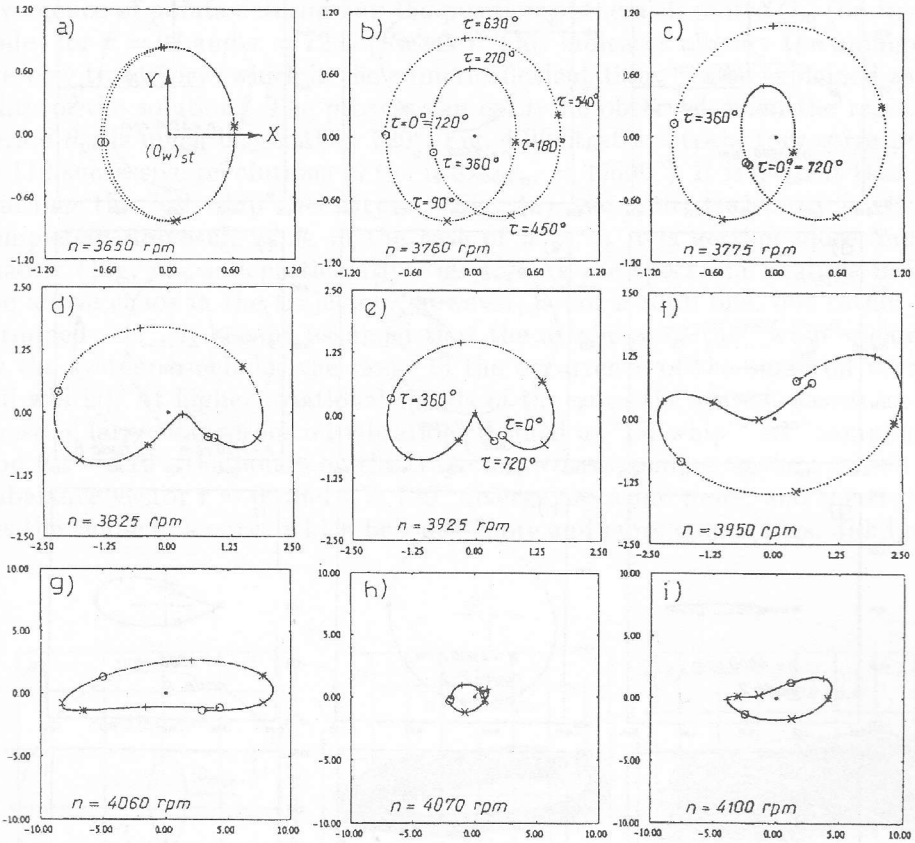

Fig. 2. Generation a), and development b), c), d) of small oil vibrations of the system (the disk centrenode No. 8 of Fig. 1b). Disk trajectories in transit phase e), f), g), h), i). "Sampling" period $\theta_{pr} = 720^o$ (two successive revolutions of the rotor.

place under conditions of a sudden change of the value of the phase angles Φ_w (Fig. 2b and 2c). The occurrence of the oil whirls (Figs. 2a,b,c and Figs. 3d,e,f) does not necessarily mean some danger for the operation of the whole system. Their amplitude rises in the initial period in an insignificant way. For this reason the vibration can undoubtedly be qualified for the so-called small oil vibrations. The above also implies that a precise determination of their occurrence (and therefore also the stability threshold of the system) is difficult. The phenomenon of the gradual "split" of the trajectory can occur within a considerable interval of the rotational speed of the rotor.

When the rotational speed is continuing to rise, the "half loop" disappears and the trajectory takes the shape of a "little shoe" pulsating rather rapidly (Figs. 2d,e,f,g,h,i). The vibration amplitude also rises significantly. At $n \cong 3925$ rpm,

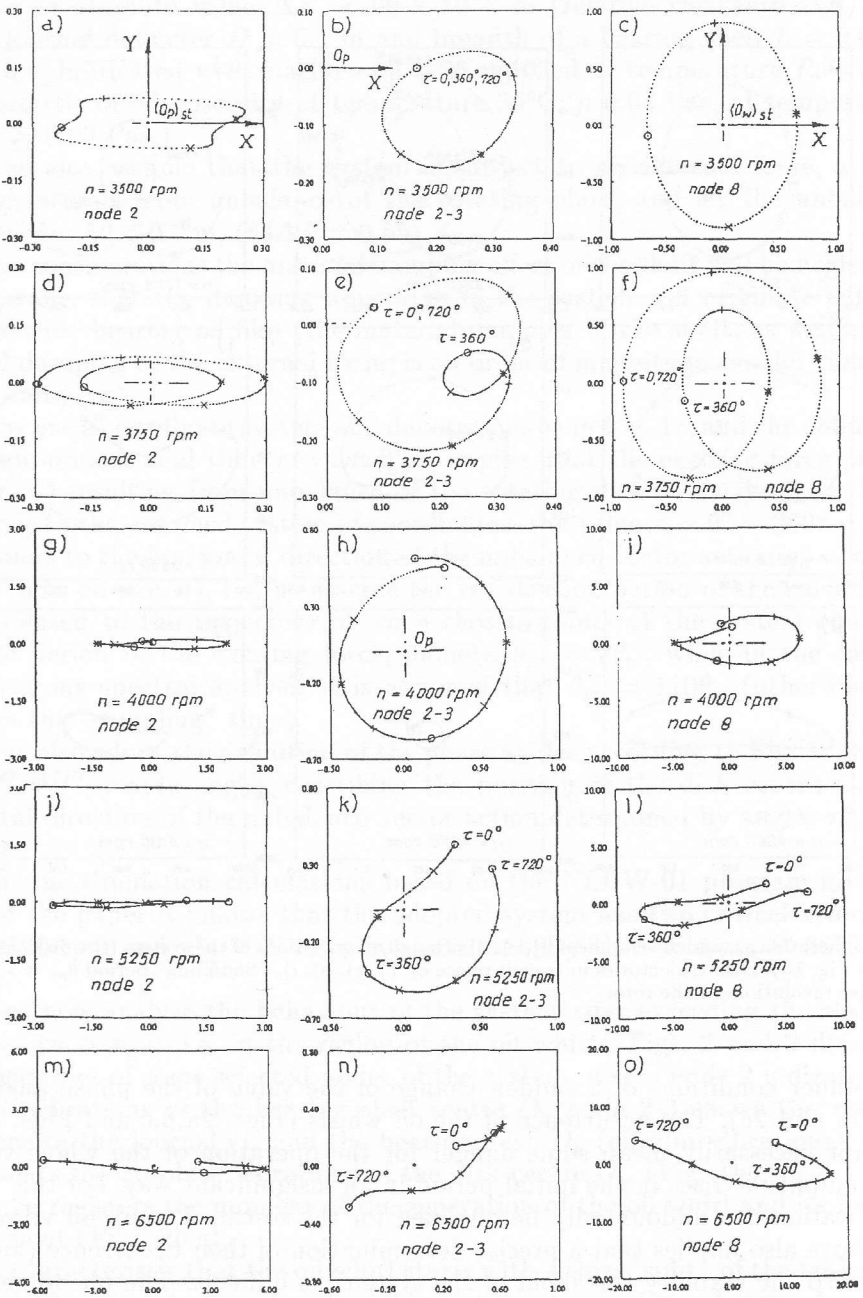

Fig. 3. Vibration trajectories of some selected nodes of the system (Fig. 1b) just before the stabi boundary a), b), c) and after exceeding it in the zone of whirls and oil "whips". "Sampling" pe $\theta_{pr} = 720°$: node 2 – absolute vibrations of the bearing shell, node 2-3 – relative vibrations of journal and the bearing shell (the oil film), node 8 – vibrations of the disk centre.

to be defined as the "whip" velocity n_b, there is initiated the process of a clear divergence of points determining the position of the disk centre O_w (or any other node) for $\tau = 0^o$ and $\tau = 720^o$ (Fig. 2e). This indicates already the ambiguity of the very trajectory (which in the numerical calculations can be explained as instability of the solution). The process can easily be observed when the registration period θ_{pr} is much bigger than 720^o. Fig. 4 illustrates a trajectory corresponding to 110 successive revolutions of the rotor ($\theta_{pr} = 39600^o$). It is evident that before reaching the "oil whip" velocity n_b (Fig. 4a), the whirl trajectory is clear and completely univocal, while in the case of $n > n_b$ it is getting more and more chaotic (Fig. 4b, and particularly Fig. 4c). As the spectrum analysis indicates, the above chaos in the trajectory, however, is not a total one, but rather a "determined one". It can be assumed that the attaining of the "whip" velocity n_b by the system concludes the range of the occurrence of the small oil vibrations (oil whirls). At higher rotational speeds of the rotor the system passes on to the phase of large, dangerous oil vibrations defined as "oil whip". At "sampling" period $\theta_{pr} = 720^o$, the points on the trajectory corresponding to the position of the unbalance vector $\tau = 0^o$ and $\tau = 720^o$ diverge more and more, and the trajectory takes the shape of a curve which becomes more and more open. (Figs. 3j,k,l,m,n,o).

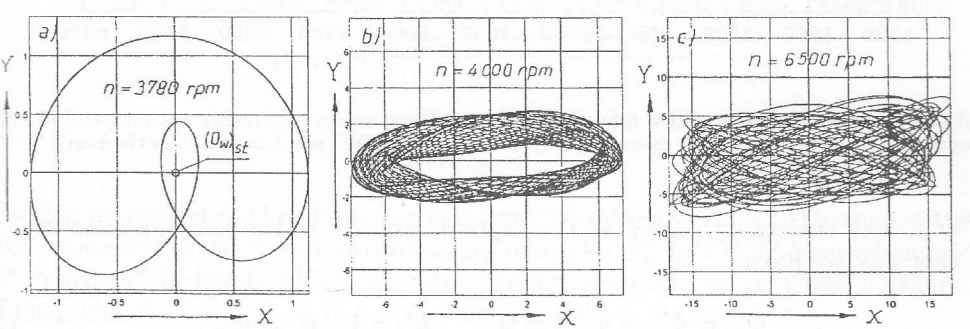

Fig. 4. Trajectories of the disk centre before reaching the "whip" velocity n_b (within the zone of small oil vibrations) – a) and after exceeding it – b), c). The "sampling" period $\theta_{pr} = 39600^o$ (110 successive revolutions).

Fig. 5 illustrates the characteristic of the amplitude centre of the disk A_w understood as a half of the greatest distance between two trajectory points, while Fig. 6 shows the phase angles Φ_w defined according to Fig. 1c. It is possible to distinguish here four characteristic zones:

Zone I – a region of a stable operation of the system – $0 < n < n_{gr}$ Some similar trajectories correspond to it, like the ones shown in Figs. 3a,b,c. Points determining the position of an arbitrary node of the system on the trajectory for $\tau = 0^o, 360^o$ and 720^o overlap accurately. Thus, the orbits indicate only one marker of rotations

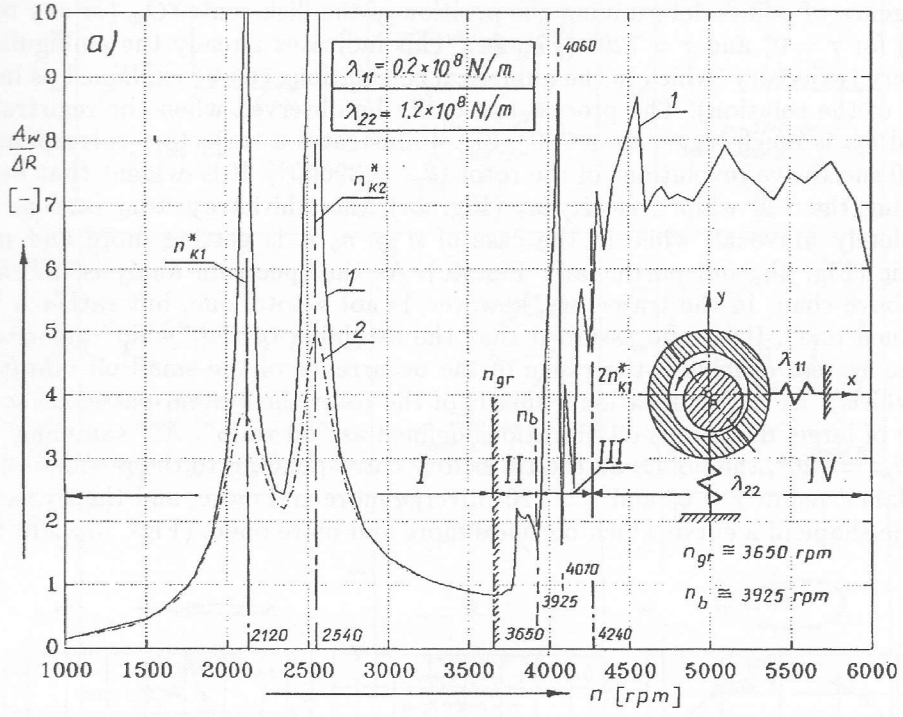

Fig. 5. Vibration amplitude of the disk centre (of node No. 8 – Fig. 1b), before reaching the stability boundary n_{gr} (zone I) and after exceeding it (zones II, III and IV – see description in the text).

$k^* = 1$. The trajectory period θ^* corresponds exactly to the exciting force θ_w. In this way we have :

$$\Phi_w = \Phi_w^0 = \Phi_w^{360} = \Phi_w^{720} \quad k^* = 1 \quad \theta^* = \theta_w. \tag{1}$$

Zone II – a zone of small oil vibrations (oil whirls) – $n_{gr} < n < n_b$ The trajectories possess a characteristic "half - loop" shape similar to the ones presented in Figs. 2a,b,c and Figs. 3d,e,f. The system has, in fact, exceeded the stability boundary n_{gr}, but the trajectories although of a different shape and period θ^*, are still stable. There takes place a clear division of the phase angles for $\tau = 0^o$ and 360^o (Fig. 6), which causes that the orbit shows the existence of two markers k^*. Thus we have :

$$\Phi_w^0 = \Phi_w^{720} \quad \text{and} \quad \Phi_w^{360} \quad k^* = 2 \quad \theta^* = 2\theta_w. \tag{2}$$

Zone III – a transition zone – $n_b < n < 2n^*_{k1}$ The "oil whip" speed n_b has been exceeded in the system, the trajectories become unstable (Figs. 4b, and Figs. 2e,f,g,h,i,j; Figs. 3g,h,i), observed there are high amplitude oscillations and a

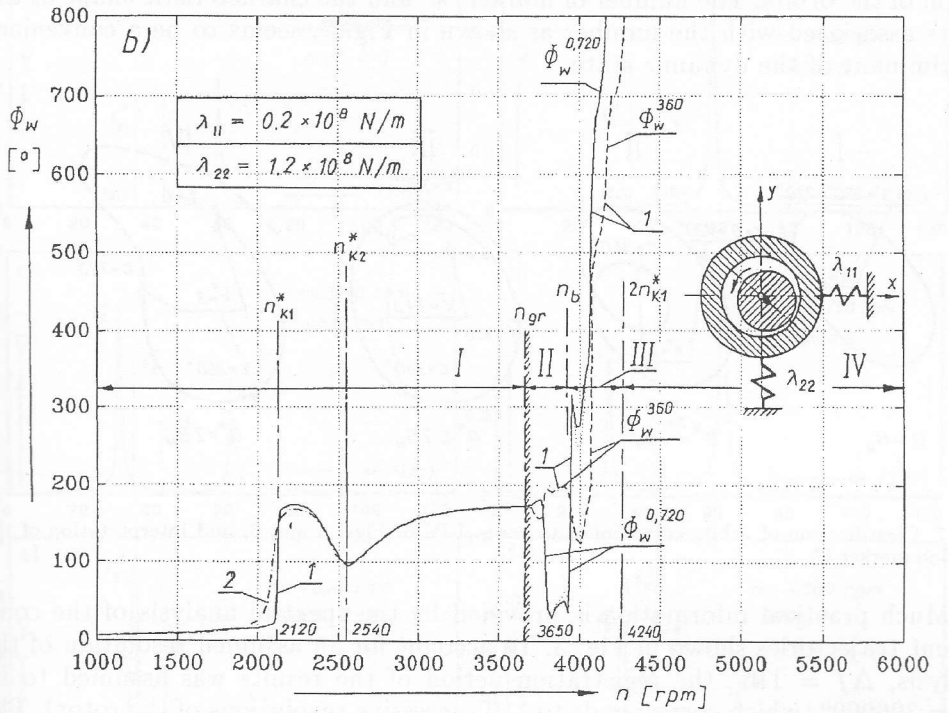

Fig. 6. Phase angles of the disk centre according to their definition of Fig. 1c. Meaning of zones I-IV and denotations as in Fig. 5.

sudden increment of the phase angles magnitude (Figs. 5 and 6). There is initiated the process of division and also rejoining of angles Φ_w^0 and Φ_w^{720} even when period θ^* "shrinks" in itself, which indicates the existence of two or three markers k^*. Thus, we have :

$$\Phi_w^0 = \Phi_w^{720} \quad \text{and} \quad \Phi_w^{360} \quad k^* = 2 \quad \theta^* = 2\theta_w \tag{3a}$$

or

$$\Phi_w^0, \Phi_w^{360}, \Phi_w^{720} \quad k^* = 3 \quad \Theta^* < 2\theta_w. \tag{3b}$$

Zone IV – a zone of intensive oil vibrations (developed oil "whip") – $n > 2n^*_{k1}$ The trajectories have a chaotic shape (Fig. 4c), the points for $\tau = 0°$ and $720°$ are distinctly separated (Figs. 3j,k,l,m,n,o), which suggests the existence of three markers k^* on the orbits (at "sampling" period $\theta_{pr} = 720°$). Thus:

$$\Phi_w^0, \Phi_w^{360}, \Phi_w^{720} \quad k^* = 3 \quad \theta^* > 2\theta_w. \tag{4}$$

From the carried out simulation investigation it is possible to draw a conclusion concerning the operational conditions of the system by appropriate classifi-

cation of the orbits. The number of markers k^* and the characteristic shape of the orbits associated with the number as shown in Fig. 7, seems to be a convenient discriminant of the dynamic state.

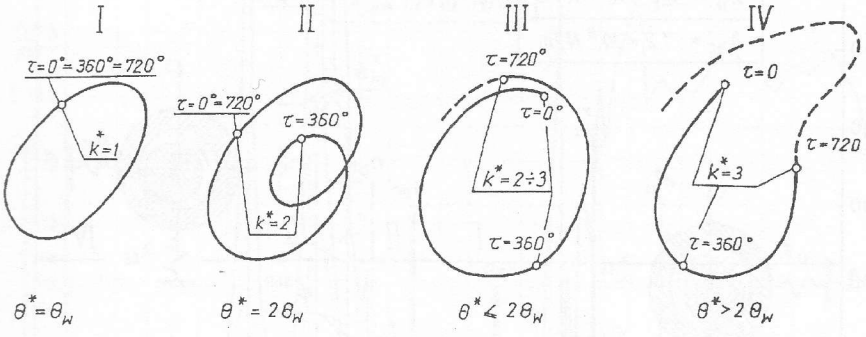

Fig. 7. Classification of arbits corresponds to zones I-IV of Figs. 5 and 6, and interpretation of the rotation marker k^*.

Much practical information is provided by the spectral analysis of the component trajectories shown in Fig. 3. To account for an assumed resolution of the analysis, $\Delta f = 1\text{Hz}$, the registration period of the results was assumed to be $\theta_{pr} = 396000^\circ$ (which corresponds to 110 successive revolutions of the rotor). The calculated results performed using the fast Fourier transform (FFT) are presented in Fig. 8.

When the stability boundary has been exceeded (Fig. 8c,d) it is possible to notice a characteristic subharmonic spectral line of frequency $f_s^* \cong 0.5 f_n$. The spectral line, in relation to the whole spectrum structure, indicates the influence of the oil film properties of the bearings, and in this way also the share of the self-excited vibrations in the image of the entire system vibrations. As the rotational speed of the rotor rises, its amplitude increases approaching asymptotically the first critical frequency of the system f_{k1}^*, where the relationship $f_s^* \cong 0.5 f_n$ is retained (hence sometimes is also used the term "half-frequency vibrations"). After exceeding the "whip" velocity n_b, there appears the second subharmonic spectral line f_{s2}^* tending asymptotically towards the other critical frequency of the system f_{k2}^*. The first spectral line f_{s1}^* stabilizes its position without exceeding the frequency (Figs. 8g,h,i,j), though the synchronous frequency f_n increases. The above takes place when $f_n > 2f_{k1}^*$ $(n > 2n_{k1}^*)$, that is, in the region of large oil vibrations (oil "whip").

The performed spectral analysis shows an interesting possibility of the subharmonic spectral line f_s^* to split into two spectral lines f_{s1}^* and f_{s2}^* (in more complex cases there is even likely to occur a disintegration into several spectral lines). The spectral line becomes dominant within the entire structure of the spectrum, which means, that the slide bearings, in principle, generate energy necessary to maintain vibrations of the whole system.

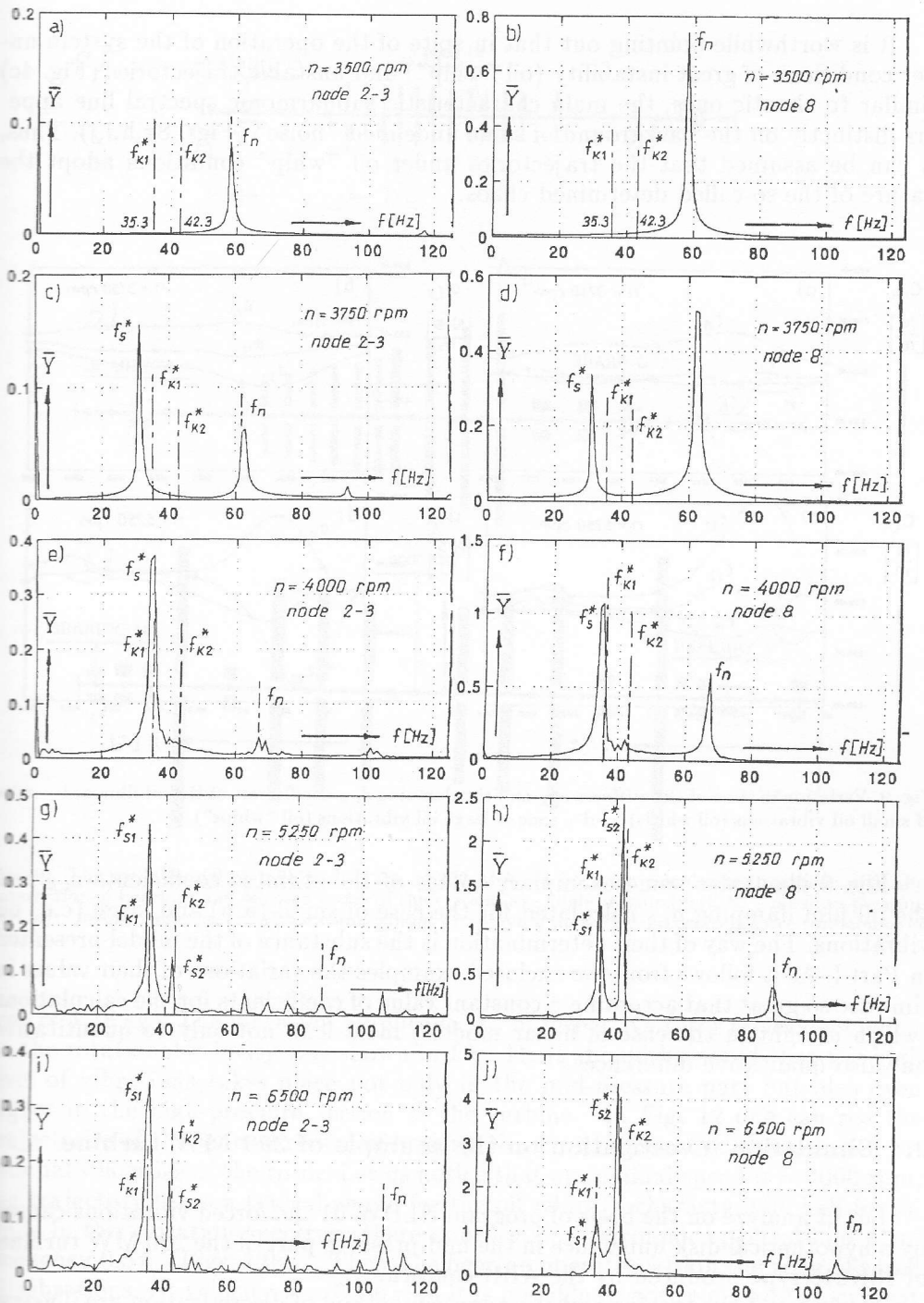

g. 8. Vibration spectra of the vertical component $Y(t)$ of the journal trajectory in relation to the aring shell (nodes 2-3), and the disk centre (node 8) before reaching the stability boundary a), b) and er exceeding it c) – j).

It is worthwhile pointing out that in spite of the operation of the system under conditions of great instability (oil "whip") and unstable trajectories (Fig. 4c similar to chaotic ones, the main characteristic subharmonic spectral line appears distinctly on the background of some undefined "noise" (Figs. 8g,h,i,j). Thus it can be assumed that the trajectories under oil "whip" conditions adopt the nature of the so-called determined chaos.

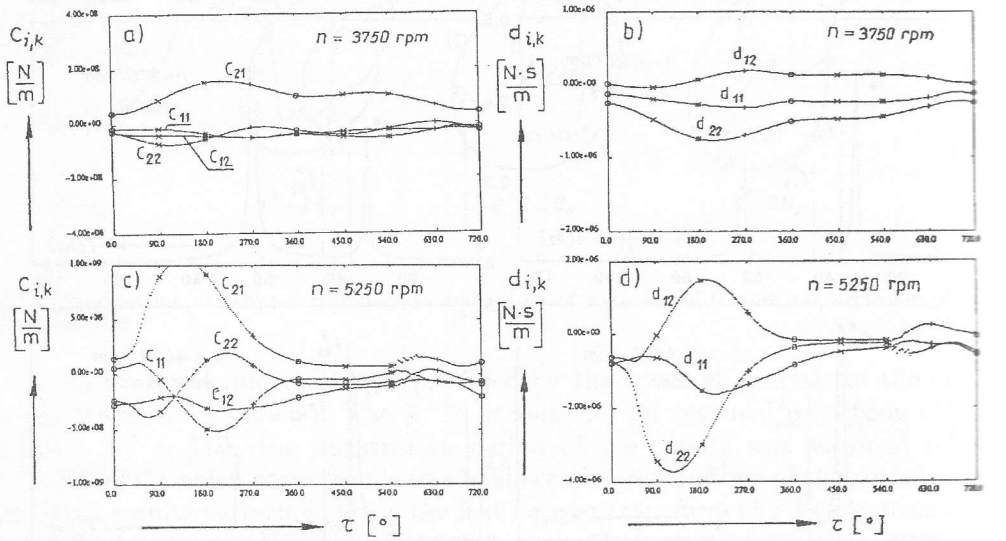

Fig. 9. Variation in time of the stiffness $c_{i,k}$ and the damping $d_{i,k}$ coefficients of the oil film. a, b – zone of small oil vibrations (oil whirls), c, d – zone of large oil vibrations (oil "whips").

Fig. 9 illustrates some exemplary values of the stiffness coefficients $c_{i,k}$ and the oil film damping $d_{i,k}$ calculated for the case of small (a,b) and large (c,d) oil vibrations. The way of their determination is the substance of the model presented in Part I. As it follows from the enclosed examples the variations of their values in time are so great that accepting a constant value of coefficients for the calculations (which is right in the case of linear models) must lead not only to quantitative but also qualitative differences.

3. Simulation investigation on the example of 200 MW turbine

Let us analyze on the basis of program NLDW-01 the forced vibrations caused by a hypothetical disk unbalance in the mid-pressure part of the 200 MW turbine of 13K215 type produced by the ABB concern.

A scheme of the turbine and the adopted method of discretization are illustrated in Fig. 10. Let the magnitude of the unbalance force q_n (Fig. 10b) results from the assumed mass of unbalance, approximately equal to the mass of one blade

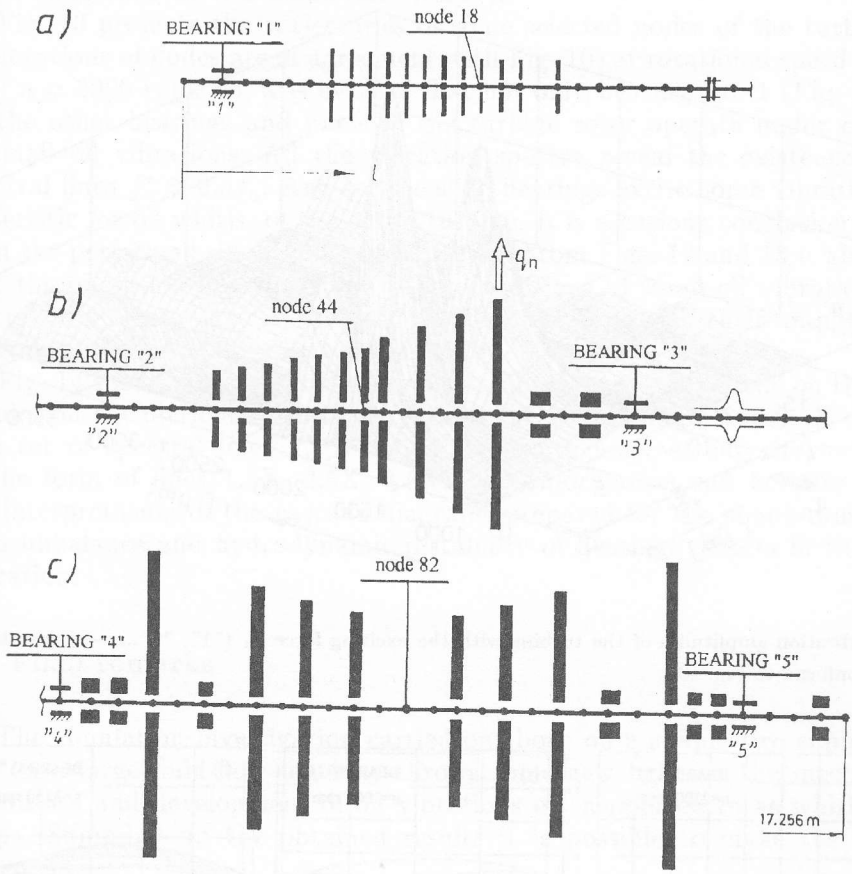

Fig. 10. The rotor model of turbine 13K215 of 200 MW adopted for calculations together with the enumeration of bearings and selected nodes of the system: a) – high-pressure part, b) – medium-pressure part, c) – low-pressure part of the turbine – point of applying the vibration exciting force (unbalance of stage).

(m_n = 3.38 kg). The vibration amplitude A_w of respective rotor nodes depending on the rotational velocity n is shown in Fig. 11. It should be noted that the high level of vibrations takes place not only in the mid-pressure part but also even higher in the high-pressure section of the turbine. In Fig. 12 one can see the trajectories of the journal centre of bearing No. 1 with respect to three chosen rotational velocities of the rotor. Let us notice that at nominal speed n = 3000 rpm, the trajectory takes a typical shape for the oil whirl (a characteristic half-loop), while in the vibration spectrum there appears a subharmonic spectral line f_s^* of frequency $0.5f_n$ (Figs. 12b,c). Thus, the bearing operates within the zone of small oil vibrations. At velocity n = 3250 rpm it is possible to notice already an evident unstable trajectory, and the bearing has attained the "oil whip" velocity n_b. The turbine, increasing gradually the rotational speed, can then enter the stage of

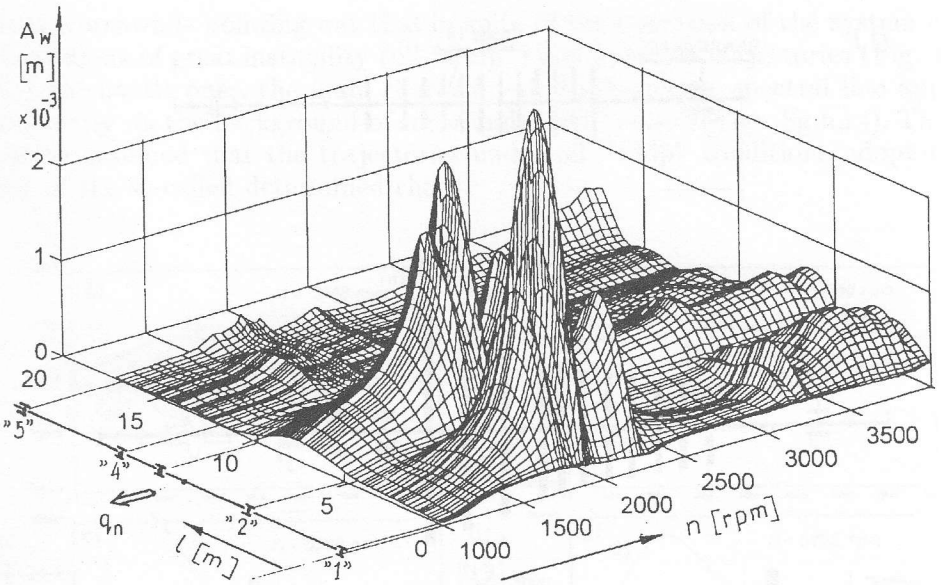

Fig. 11. Vibration amplitudes of the turbine with the exciting force q_n ("1", "2".... – numeration of bearings conforms to Fig. 10).

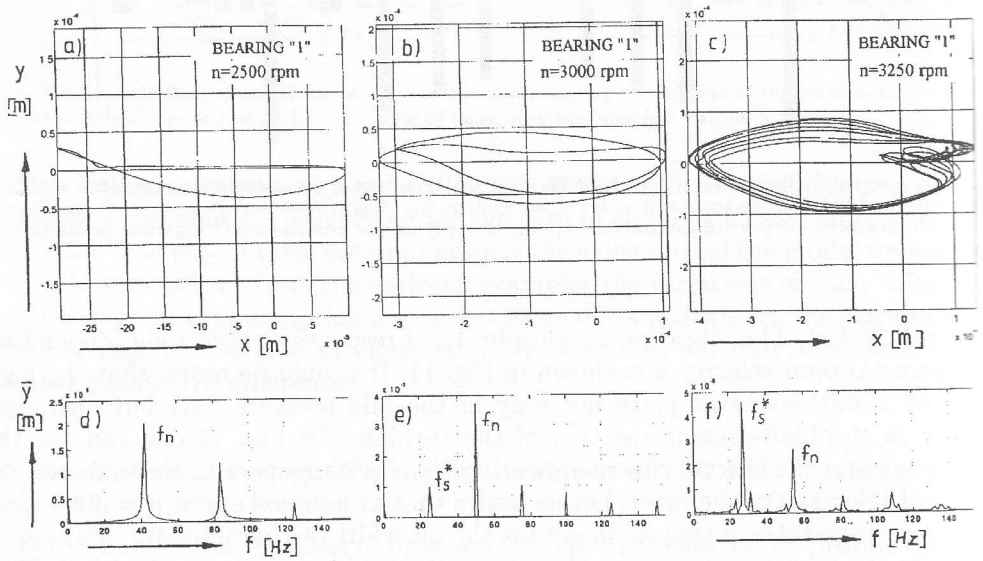

Fig. 12. The journal trajectories in bearing "1" and the vibration spectra of component $y(t)$ for three different rotational speeds of the turbine: a), d) – the case of stable vibration, b), e) – the case of small oil vibrations, c), f) – the case of attaining the "whip" velocity.

large, dangerous oil vibrations (oil "whip").

Fig. 13 presents the trajectories of some selected nodes of the turbine rotor (denotations of nodes are in agreement with Fig. 10) at rotational speed (nominal one) $n = 3000$ rpm. So, it is evident that not only bearing No. 1 (Fig. 12b), but all the other bearings and parts of the turbine rotor operate under conditions of small oil vibrations. All the vibration spectra reveal the existence of some spectral lines $f_s^* \cong 0.5 f_n$. And so, the slide bearings excite some vibrations, characteristic for oil whirls, of the entire turbine. It is a curious conclusion resulting from the performed simulation investigation. From Figs. 12 and 13 it also follows that the operation of the turbine under conditions of small oil vibrations is not particularly dangerous. The trajectories become stable and their amplitudes rise insignificantly (compare Figs. 12a and 12b).

Fig. 14 shows a cascade diagram of the vibration spectra made on the base of simulation calculations for bearing No. 1. The subharmonic line 0.5X consisting of a set of spectral lines $f_s^* \cong 0.5 f_n$, has quite unexpectedly its own "echo" in the form of lines 1.5X, 2.5X, 3.5X. This information can become useful in the interpretation of the cascade diagrams prepared for the simulation of other than unbalance and hydrodynamic instability of bearings defects in the turbine operation.

4. Final remarks

The simulation investigation carried out both on a simple two-support rotor and on a large fluid-flow machine throws some new light on the mechanism of generation and development of oil vibrations often referred to as whirls and oil whips. Summing up the obtained results it is possible to make the following statements:

- The oil whirls are generated in the process of slow trajectory "splitting" into two loops of which one is decreasing with the rise of velocity until complete fading. The trajectory remains stable, whereas its amplitude rise is moderate. The spectral analysis indicates the existence of a subharmonic spectral line with the frequency $f_s^* \cong 0.5 f_n$, which means that the oil film in the bearings generates vibrations of frequency equivalent (approximately) to the half of the synchronous one. This stage of the system self-excited vibrations can be defined as small oil vibrations (or half-frequency vibrations).

- It is possible to distinguish a certain characteristic velocity n_b (defined in the paper as "whip" velocity). As soon as this velocity has been exceeded the trajectories loose their stability, and their amplitude starts rising abruptly. There is also possible a process of splitting the subharmonic spectral line into two spectral lines (or more). The effect of the bearing properties upon the operation of the system becomes more and more complicated, and at the same time, dominant. This operating region can be described as a transient phase between small and large oil vibrations.

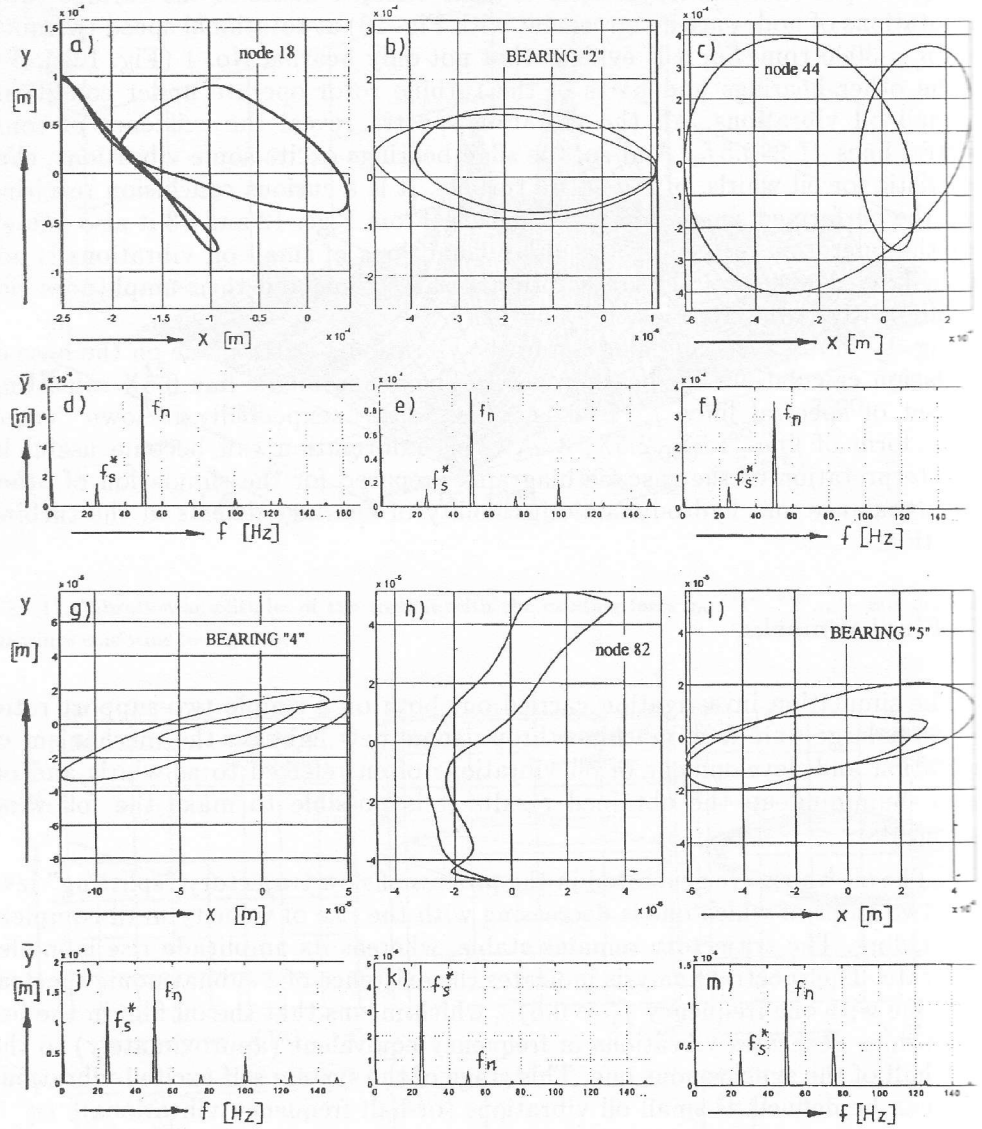

Fig. 13. Trajectories of selected nodes of the turbine and vibration spectra of component $y(t)$ (numeration of nodes and bearings conforms to Fig. 10) with respect to nominal speed $n = 3000$ rpm.

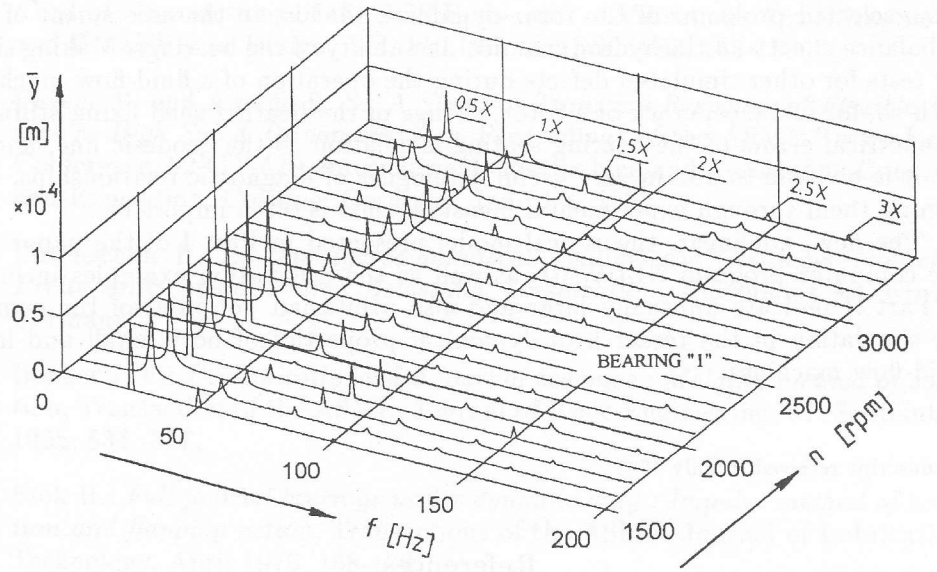

Fig. 14. Cascade diagram of vibration spectra of bearing "1" (for component $y(t)$).

- When the double of primary critical velocity has been exceeded by the system, the vibration amplitude of the system gradually stabilizes at a very high level. The subharmonic spectral line, definitely dominant in the spectrum structure, also stabilize its position at the level of critical frequency. The trajectories become chaotic (but determined). This stage of vibrations can be described as large oil vibrations (oil "whip").

- When the registration period of the results is equal to the double period of the synchronous excitation functions ($\theta_{pr} = 2\theta_w$), the above development phases of the self-excited oil vibrations can be identified on the basis of the proposed orbit classification. A useful diagnostic factor here can be the number of the rotation markers k^* (Fig. 7).

- A significant unbalance of the rotor, also with respect to large turbine sets can be responsible for situations when the slide bearings force some characteristic oil vibrations, (very often small vibrations, that is whirls) involving the entire machine (Fig. 13). The trajectories, in general, remain stable, and their amplitude rises insignificantly in spite of the fact that the system has really exceeded the stability threshold. Such a state in numerous cases can be regarded as a normal situation fluid-flow machine operation.

The results of the simulation investigation presented in the paper refer to some selected problems of the rotor dynamics, that is, to the assessment of the unbalance effect and the hydrodynamical instability of the bearings. Making similar tests for other simulated defects during the operation of a fluid-flow machine, such as, for instance, crack of a rotor, change of the bearing shell fixing stiffness, geometrical errors of the bearing seating in relation to the geodesic line, and so on, it is possible to obtain very useful catalogues of diagnostic relationships. Obtaining them through experimental measurements is often impossible.

The new, nonlinear, theoretical model presented in Part I of the paper and the computer program NLDW-01, as well as the calculation examples included in Part II indicate unusually large and also utilitarian potential of the computer simulation in the research of dynamical properties of both small and large fluid-flow machines.

Manuscript received in July 1995

References

[1] Hori Y.:*A theory of oil whip*, Transactions of the ASME, Journal of Applied Mechanics, June 1959, 189-198.

[2] Muszyńska A.: *Whirl and Whip-Rotor/Bearing Stability Problems*, Journal of Sound and Vibrations, 110(1986), No. 3.

[3] Khonsari M. M. and Chang Y. J.: *Stability Boundary of Nonlinear Orbits Within Clearance Circle of Journal Bearings*, Transactions of the ASME, Journal of Vibration and Acoustics, Vol. 115, July 1993, 303-307.

[4] Subbiah R. and Rieger N. F.: *On the Transient Analysis of Rotor-Bearing Systems*, Transactions of the ASME, Journal of Vibration, Acoustics, Stress and Reliability in Design, Vol. 110, October 1988, 515-520.

[5] Ding J. and Krodkiewski M.: *Inclusion of static indetermination in the mathematical model for nonlinear dynamic analyses of multi-bearing rotor system*, Journal of Sound and Vibration, 164(1993), 267-280.

[6] Russo M and Russo R.: *Parametric excitation instability of a rigid unbalanced rotor in short turbulent journal bearings*, Proc. Instn. Mech. Engrs., Part C : Journal of Mechanical Engineering Science, 207(1993), 149-160.

[7] Hattori H. and Kawashima N.: *Dynamic Analysis of a Rotor-Journal Bearing System with Large Dynamic Loads*, JSME International Journal, Series III, 34(1991), No. 4, 503-511.

[8] Muszyńska A., Franklin W. D. and Bently D. E.: *Rotor Active "Anti-Swirl" Control*, Transactions of the ASME, Journal of Vibration, Acoustics, Stress and Reliability in Design, Vol. 110, No. 2, April 1988, 143-150.

[9] Pavelic V. and Amano R. S.: *A Study of Transient Response of Flexible Rotors in High Speed Turbomachinery*, Proceedings of the ASME Turbo-Expo Conference, 92-GT-420, International Gas Turbine and Aeroengine Congress and Exposition, Cologne, Germany, June 1-4, 1992.

[10] Butenschön H. J.: *Das hydrodynamische zylindrische Gleitlager endlicher Breite unter instationärer Belastung*, Dissertation, Universität Karlsruhe, Germany.

[11] Booker J. F.: *Dynamically loaded journal bearings : Mobility method of solution*, Transaction of the ASME, Journal of Basic Engineering, 87, September 1965, 534 -537.

[12] Blok H.: *Full journal bearings under dynamic duty : Impulse method of solution and flapping action*, Transactions of the ASME, Journal of Lubrication Technology, April 1975, 168-179.

[13] Kiciński J.: *Influence of the flow prehistory in the cavitation zone on the dynamic characteristics of slide bearings*, Wear, 111(1986), 289-311.

[14] Kiciński J.: *New method of description of dynamic properties of slide bearings*, Wear 132, 1989, 205-220.

[15] Kiciński J.: *The Influence of Thermoelastic Deformations of Bearing Bush and its External Fixings on Static and Dynamic Properties of Journal Bearings. Part I and II*, Transaction of the Institute of Fluid-Flow Machinery, 93(1991), 163-194.

[16] Kiciński J. and Materny P.: *Modelling of the dynamic interactions of the complex rotor-supports system*, Machine Dynamics Problems, 5(1993), 7-28.

Nieliniowy model drgań w układzie wirnik-łożyska
Część II. Wyniki obliczeń

Streszczenie

W pracy przedstawiono wyniki badań symulacyjnych odnoszące się do opisu najbardziej frapujących ciągle nie wyjaśnionych do końca zjawisk zachodzących w filmie olejowym łożysk ślizgowych, a mianowicie wirów olejowych i bicia olejowego. Zjawiska te, określane też terminem małych i dużych drgań olejowych, wywołują drgania samowzbudne całego układu wirnik-łożyska. Badania symulacyjne przeprowadzone zostały w oparciu o model teoretyczny i algorytm obliczeń, przedstawione w części I pracy.

Obliczenia przeprowadzono na przykładzie laboratoryjnego wirnika dwupodporowego z podatnymi utwierdzeniami zewnętrznymi panwi, a także na przykładzie wirnika turbiny parowej o mocy 200 MW. Zamieszczone zostały wyniki obliczeń w postaci trajektorii wybranych punktów układu po przekroczeniu

granicy stabilności, przebiegów amplitud i kątów fazowych, a także w postaci widm drgań. Przeprowadzono obszerną dyskusję uzyskanych wyników. Określone zostały szczegółowo poszczególne fazy rozwoju drgań olejowych oraz podjęta została próba klasyfikacji orbit i wprowadzenia użytecznego wyróżnika diagnostycznego.